Journal of Molecular Structure 1265 (2022) 133441

Contents lists available at ScienceDirect

Journal of Molecular Structure

journal homepage: www.elsevier.com/locate/molstr

Design, synthesis, biological activity evaluation and *in silico* studies of new nicotinohydrazide derivatives as multi-targeted inhibitors for Alzheimer's disease

Fatih Tok[a,*], Begüm Nurpelin Sağlık[b,c], Yusuf Özkay[b,c], Zafer Asım Kaplancıklı[b], Bedia Koçyiğit-Kaymakçıoğlu[a]

[a] Department of Pharmaceutical Chemistry, Faculty of Pharmacy, Marmara University, 34854, Istanbul, Turkey
[b] Department of Pharmaceutical Chemistry, Faculty of Pharmacy, Anadolu University, 26470, Eskişehir, Turkey
[c] Doping and Narcotic Compounds Analysis Laboratory, Faculty of Pharmacy, Anadolu University, 26470, Eskişehir, Turkey

ARTICLE INFO

Article history:
Received 17 March 2022
Revised 20 May 2022
Accepted 2 June 2022
Available online 3 June 2022

Keywords:
Alzheimer's disease
Beta-amyloid plaque
Beta secretase
Cholinesterase inhibitors
Hydrazone
Molecular docking

ABSTRACT

A new series of 6–chloro-*N*'-(substituted benzylidene)nicotinohydrazide were synthesized *via* condensation reactions between the corresponding hydrazides and aldehydes**.** All compounds were tested for their AChE and BuChE inhibitory activity. Compounds **P5, P7, P9, P10** and **P12** exhibited significant AChE inhibition potencies. Among them, compound **P5** having para nitro substituent was found to be the most effective derivative against AChE with an IC_{50} value of 0.027 ± 0.001 µM. After that, the BACE-1 and beta-amyloid plaque inhibitory potencies of selected compounds **P5, P7, P9, P10** and **P12** were evaluated. Among them, compound **P5** displayed the highest inhibition rate against the BACE-1 enzyme and beta-amyloid plaque. Molecular docking studies were carried out using both AChE and BACE-1 crystals to determine the compound's interactions with the enzyme's active sites. Furthermore, we evaluated the ADMET properties of compounds and their blood–brain barrier (BBB) permeation was also found to be high.

1. Introduction

Alzheimer's disease (AD) is a genetic and sporadic neurodegenerative illness characterized by cognitive impairments in expressive speech, visuospatial processing and executive (mental agility) functions [1]. The prevalence of AD estimates 10–30% in the population >65 years of age with an incidence of 1–3% [2]. The most important changes detected in the pathogenesis of AD are senile plaques composed of extracellular deposits of amyloid-β (Aβ), neurofibrillary tangles formed by tau protein accumulation and reactive glial-microglial changes [3,4].

The cholinergic deficits in AD is one the major pathogenesis cause leading to learning and memory loss [5]. Acetylcholine is broken down or hydrolyzed by the AChE into choline and acetic acid [6]. This is a critical way for the synaptic transmission and preventing continuous nerve firings at nerve endings [7]. AChE inhibitors are one of the most important approaches in the treatment of AD by increasing synaptic levels of acetylcholine [8,9]. There are a limited number of drugs approved for the treatment of AD by the FDA, such as donepezil, galantamine, and rivastigmine [10]. The development of new AChE inhibitors is an immediate necessity.

One of the AD pathologies is the abnormal deposition of proteins inside and outside of brain cells [11]. Abnormal accumulation of amyloid forms toxic Aβ aggregates, leading to the formation of senile plaques and neurofibrillary tangles, two of the pathological features of AD [12].

Amyloid β (Aβ) accumulation results from the abnormal processing by α-secretase, β-secretase (BACE1) and γ-secretase enzymes [13,14]. Aβ deposition can be prevented by BACE1 inhibition [15]. BACE1 is the main drug target for inhibition of Aβ production in AD. Recent findings revealed that AChE is associated with diffuse pre-amyloid deposits and mature amyloid plaques in an AD patient's brain. It also induces Aβ fibrillogenesis through the formation of stable Aβ-AChE complexes. Neurons treated with these complexes show a more impaired appearance compared to neurons treated with Aβ alone [16]. Therefore, having both AChE and

* Corresponding author. Department of Pharmaceutical Chemistry, Faculty of Pharmacy, Marmara University, Istanbul 34854, Turkey.
E-mail address: fatih.tok@marmara.edu.tr (F. Tok).

https://doi.org/10.1016/j.molstruc.2022.133441
0022-2860/

BACE1 inhibitory properties while designing drugs is an important approach for the treatment of AD.

Nitrogen-containing heterocyclic structures have a wide range of biological activities [17]. A large number of highly active compounds bearing a pyridine ring are available for the treatment of AD in the literature [18–20]. On the other hand, hydrazone structures demonstrated good AChE inhibitory activity [21–23]. Because hydrazone structure can interact with target enzymes and receptors by having both nucleophilic and electrophilic properties with its unique -C=N–NH- pharmacophore group [24].

The crystal structure of AChE reveals that it has a peripheral anionic domain (PAS) and a catalytic active site (CAS) [25]. Studies showed that AChE inhibitors must include the following structural requirements. (i) A ring system that can interact with PAS, (ii) a basic center that can bind to CAS, and (iii) a linker such as -O-, CH_2, CONH, and CONH(CH_2)n that acts as a bridge between this ring system and the basic center [26].

Donepezil molecule consists of three different parts: an aromatic system, a linker and a basic center [27,28]. In this study, the pyridine ring (a six-membered heteroaromatic ring) bearing chloro substituent was chosen as the aromatic ring system instead of an indanone core ring in donepezil. As the linker, the hydrazone structure was preferred instead of the methylene residue in donepezil. Thus, the designed molecule had the flexibility and the ability to make additional hydrogen bonds with AChE due to the hydrazone structure. The benzylidenehydrazine moiety was preferred as the basic center instead of the benzylpiperidine ring in donepezil. In addition, different substituents on this benzylidenehydrazine group were considered to compare the effect of electron-donating or withdrawing groups on the activity. Taking these facts into account, we designed new hydrazone derivatives bearing pyridine ring and investigated their cholinesterase, β-secretase and beta amyloid plaque inhibitory activity against AD (Fig. 1).

2. Result and discussion

2.1. Chemistry

Hydrazone derivatives were obtained according to the synthesis pathway given in Scheme 1. Firstly, *6-chloronicotinohydrazide* was prepared by reflux of ethanolic solutions of *methyl 6-chloropyridine-3-carboxylate* and hydrazine monohydrate. Hydrazide compound was reacted with substituted benzaldehyde derivatives by heating in order to get target compounds (**P1**-**P12**). The structures of synthesized compounds were proved by using IR, ^{1}H NMR, ^{13}C NMR and elemental analysis.

In the IR spectrum, the band at 3144–3419 cm^{-1} was assigned to the N–H stretching mode of the hydrazone group. In addition, the bands corresponding to the C=O and C=N stretching modes were observed in the range of 1633–1697 cm^{-1} and 1599–1640 cm^{-1}, respectively. In the ^{1}H NMR spectrum, ortho, meta and para protons belonging to the pyridine ring were detected separately. The hydrogen atoms at the meta position in pyridine resonated as a doublet peak at 7.60–7.72 ppm due to the shielded effect. Hydrogen atoms at the para position are less affected and recorded as a doublet at 8.27–8.33 ppm. The ortho protons of pyridine were also deshielded and found at 8.89–8.92 ppm because of the withdrawing properties of a nitrogen atom in the pyridine ring. The NH protons of hydrazone derivatives gave as singlet peak between 8.32 ppm and 8.45 ppm. The proof for the formation of hydrazone compounds was that the peak of the azomethine protons was observed at 11.78–12.36 ppm in the spectrum. In the ^{13}C NMR spectrum, the characteristic azomethine (C=N) carbon of hydrazones and pyridine ring appeared at 149.13–149.98 and 152.63–153.29 ppm, respectively. In addition, the carbonyl (C=O) peak of hydrazone compounds was detected at 160.01–160.86 ppm.

2.2. Evaluation of biological activity studies

2.2.1. ChE enzymes inhibition

The results of BChE enzyme activity revealed that all derivatives excluding compounds **P5, P7, P9, P10** and **P12** had activity higher than 50% at 10^{-3} M concentration (Supplementary File **Table S1**). But, when the results of the activity at 10^{-4} M concentration were analyzed none of the synthesized compounds showed remarkable inhibition rates. When it was compared with the results obtained in the AChE enzyme inhibition test at these concentrations, almost all of the compounds in the series showed more selective inhibition against the AChE enzyme (Table 1-selectivity and selectivity index). The reference agent tacrine had inhibitory activity at the rate of 99.827 ± 1.378% and 98.651 ± 1.402% at 10^{-3} and 10^{-4} M concentrations (Table 1).

It was observed from AChE enzyme inhibition results that all of the obtained compounds demonstrated a high rate of activity (more than 50%) at 10^{-3} M concentrations (Supplementary File **Table S1**). Among the synthesized compounds, derivatives **P3, P5-P12** displayed a quite strong AChE enzyme inhibition profile by generating at least 80% activity. Compounds **P5, P7, P9, P10** and **P12** were selected for the second stage of the enzyme activity test by having higher than 50% inhibitory activity at 10^{-4} M concentration. Meanwhile, the reference drug donepezil had inhibitory activity at the rates of 99.254 ± 2.104% and 97.426 ± 1.890%, respectively at 10^{-3} and 10^{-4} concentrations. The further concentrations of the selected derivatives were prepared with serial dilutions for the second stage of the AChE enzyme inhibition assay (Table 1).

The IC_{50} value of donepezil was found 0.021 ± 0.001 μM on AChE enzyme; while the IC_{50} values of compounds **P5, P7, P9, P10** and **P12** were found in the range of 0.027 ± 0.001 - 0.102 ± 0.004 μM. Among these compounds, compounds **P5, P7, P9** and **P12** were found to have the strongest AChE inhibition with the lowest IC_{50} value. The IC_{50} values of compounds **P5, P7, P9** and **P12** were calculated as 0.027 ± 0.001 μM, 0.031 ± 0.001 μM, 0.037 ± 0.001 μM and 0.034 ± 0.001 μM, respectively (Table 1). The compounds **P7, P9** and **P12** demonstrated an inhibition profile with very close IC_{50} values to that of donepezil. The compound **P5** was found to be the most effective agent in the series and it displayed potent inhibitory capability very similar to donepezil.

2.2.2. β-Secretase (BACE-1) enzyme inhibition

The *in vitro* BACE-1 inhibitory potencies of selected compounds **P5, P7, P9, P10** and **P12**, which were found to be the most effective derivatives as a result of AChE inhibition assay, were evaluated by means of commercial fluorometric assay kit ("Human β-Secretase (BACE1) Inhibitor Screening Assay" kit (BioVision, Milpitas, CA, USA)). Donepezil was used as the reference drug. The selected compounds and donepezil were used with the same concentrations as in the AChE inhibition assay (10^{-3}–10^{-4} M) and the kit protocol was applied as in the user guide. The IC_{50} values of the selected compounds and donepezil were given in Table 2. According to the activity results, compound **P5** showed the most potent BACE-1 enzyme inhibitory activity with the IC_{50} value of 0.205 ± 0.008 μM. The IC_{50} value of donepezil and verubecestat were calculated as follows: 0.170 ± 0.007 μM and 0.029 ± 0.001 μM, respectively. Consequently, it was found that derivative **P5** had a similar level of BACE-1 inhibition potential with donepezil. But it was seen that this derivative did not display inhibition profile as strong as BACE-1 inhibitor verbucestat.

2.2.3. Beta-amyloid 1–42 (Aβ42) inhibitor screening study

In addition to the decrease in cholinergic transmission in Alzheimer's patients, amyloid plaque accumulation consisting of beta amyloid (Aβ) peptides can be considered among the important causes. In this study beta amyloid aggregation inhibition ac-

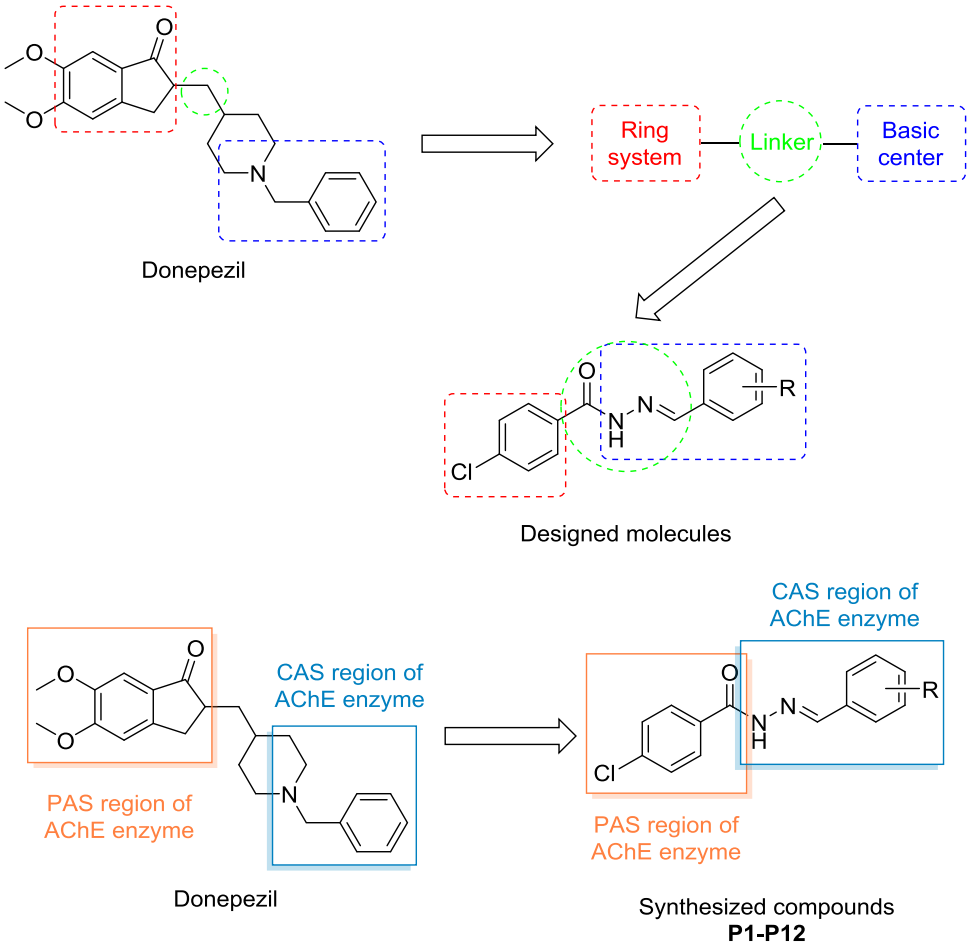

Fig. 1. The design of the synthesized compounds.

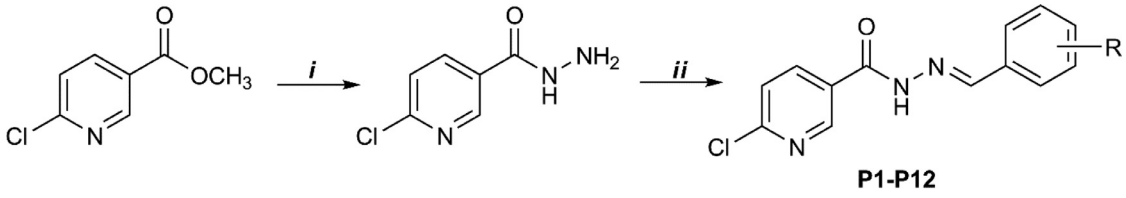

Comp.	R	Comp.	R	Comp.	R	Comp.	R
P1	4-H	**P4**	4-CH_3	**P7**	3,4-diOCH_3	**P10**	4-$COOCH_3$
P2	4-Cl	**P5**	4-NO_2	**P8**	3,4-diCl	**P11**	4-$N(CH_3)_2$
P3	4-OH	**P6**	4-F	**P9**	3-OC_2H_5-4-OH	**P12**	3-OCH_3-4-OH

Scheme 1. The synthetic route of hydrazone derivatives. Reagents: (i) hydrazine hydrate, ethanol; (ii) benzaldehyde derivatives, methanol.

tivities of compounds **P5, P7, P9, P10** and **P12**, which showed high inhibitory activity against the AChE enzyme were carried out using the "Beta-Amyloid 1–42 (Aβ42) Ligand Screening Assay (Bio-Vision, Milpitas, CA, USA)" kit based on the fluorometric method [29,30]. The test kit, based on the fluorometric method, was used in accordance with the recommended procedure. If an Aβ42 ligand is present, this reaction is inhibited/destroyed, thereby reducing or completely eliminating fluorescence. Curcumin and donepezil were used as reference drugs. Beta-amyloid plaque inhibition profiles were examined by preparing reference drugs and compounds **P5, P7, P9, P10** and **P12** at 10 μM, 1 μM, 0.1 μM and 0.01 μM concentrations. All test compound concentrations were applied in quadruplicate on the plates. When the kit protocol was completed, the% inhibition ratios of curcumin, donepezil and test compounds were calculated based on the control group. The percent inhibitions of beta amyloid 1–42 (Aβ42) peptide aggregation were given in Fig. 2.

Curcumin displayed inhibition of 92.895 ± 2.310%, 85.798 ± 2.107%, 44.740 ± 1.050% and 32.897 ± 0.970%; while,

Table 1
% Inhibition and IC_{50} values of the synthesized compounds, donepezil and tacrine against AChE and BChE.

Compounds	Human AChE% Inhibition*	AChE IC_{50} (μM)	Human BChE% Inhibition*	Selectivity	SI*
	10^{-4} M		10^{-4} M		
P1	47.452 ± 0.733	> 100	27.451 ± 0.648	AChE	>10
P2	42.617 ± 0.641	> 100	25.124 ± 0.761	AChE	>10
P3	45.194 ± 0.885	> 100	29.099 ± 0.723	AChE	>10
P4	43.835 ± 0.692	> 100	30.634 ± 0.877	AChE	>10
P5	95.067 ± 1.408	0.027 ± 0.001	41.661 ± 0.827	AChE	>3703
P6	46.167 ± 0.830	> 100	31.149 ± 0.761	AChE	>10
P7	92.434 ± 1.989	0.031 ± 0.001	40.424 ± 0.960	AChE	>3225
P8	44.521 ± 0.722	> 100	29.610 ± 0.713	AChE	>10
P9	90.548 ± 1.887	0.037 ± 0.001	42.180 ± 0.848	AChE	>2702
P10	85.032 ± 1.133	0.102 ± 0.004	43.851 ± 0.702	AChE	>980
P11	48.875 ± 0.958	> 100	27.588 ± 0.834	AChE	>10
P12	91.247 ± 1.407	0.034 ± 0.001	40.908 ± 0.953	AChE	>2941
Donepezil	97.426 ± 1.890	0.021 ± 0.001	–	–	–
Tacrine	–	–	98.651 ± 1.402	–	–

SI*: Selectivity index (SI=IC_{50} BChE/ IC_{50} AChE).
* Human acetylcholinesterase (CAS No: 9000–81–1) and human butyrylcholinesterase (CAS No: 9001–08–5).

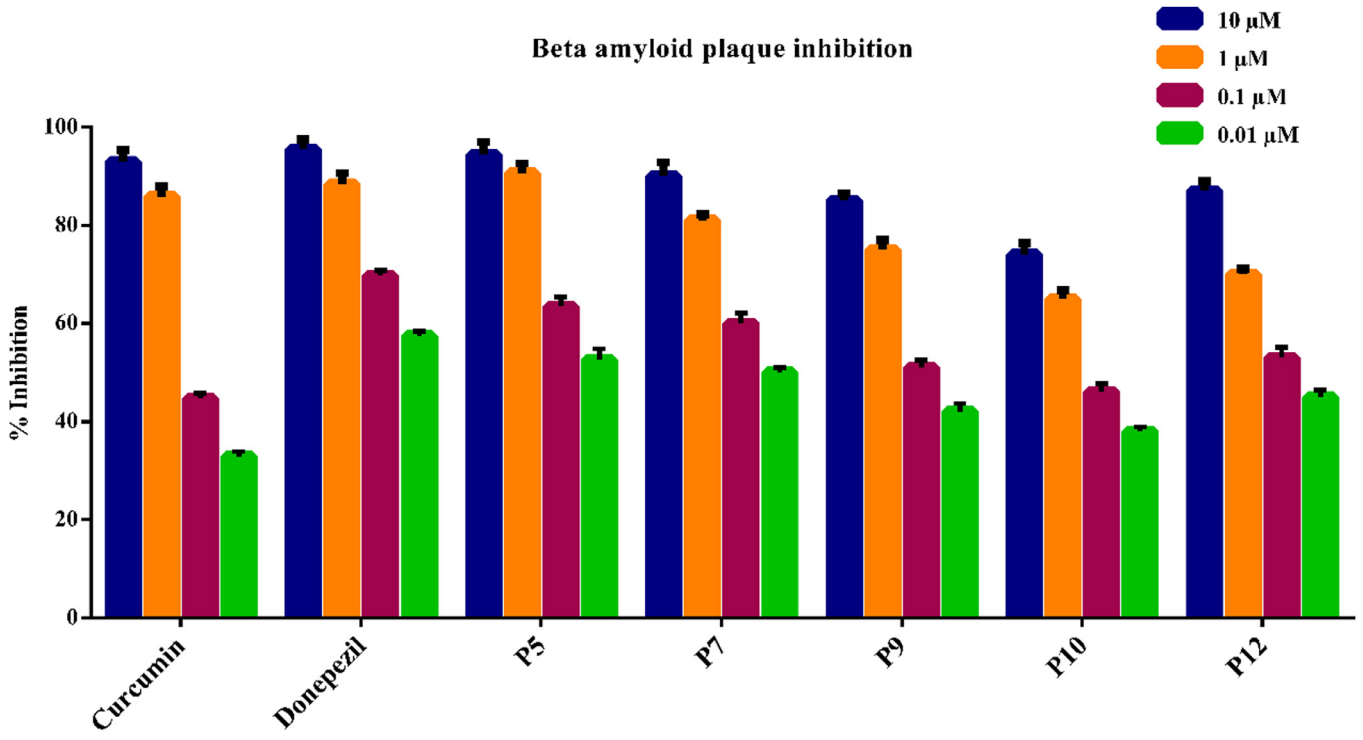

Fig. 2. Beta amyloid plaque inhibition (%) of curcumin, donepezil and compounds **P5**, **P7**, **P9**, **P10** and **P12**.

Table 2
The IC_{50} values of compounds **P5**, **P7**, **P9**, **P10** and **P12** against BACE-1.

Compounds	β-Secretase (BACE1) IC_{50} (μM)
P5	0.205 ± 0.008
P7	0.428 ± 0.016
P9	0.742 ± 0.030
P10	2.895 ± 0.103
P12	0.698 ± 0.031
Donepezil	0.170 ± 0.007
Verubecestat	0.029 ± 0.001

donepezil had inhibition 95.467 ± 2.025%, 88.340 ± 2.237%, 69.741 ± 1.033% and 52.488 ± 0.895% at 10 μM, 1 μM, 0.1 μM and 0.01 μM concentrations, respectively. More than 50% inhibition was seen in all tested compounds at concentrations of 10 μM and 1 μM. For 0.1 μM concentration, all obtained derivatives except for compound **P10** showed more than 50% inhibitor activity. Also, only compounds **P5** and **P7** were found to display more than 50% inhibitor activity at 0.01 μM concentration. Corresponding to Fig. 2, compound **P5** was determined to have the highest inhibition rate among the tested derivatives. This compound showed inhibition at related concentrations as follows: 94.317 ± 2.632%, 90.578 ± 2.017%, 63.471 ± 1.922% and 52.616 ± 1.236%, respectively. Also, it was seen that compound **P5** displayed higher inhibition than curcumin; whereas it displayed an inhibition profile at a similar rate with donepezil.

These findings indicate that the related compounds have the ability to inhibit beta-amyloid plaque aggregation in varying proportions in addition to their AChE enzyme inhibitory potentials. Preventing the accumulation of beta amyloid plaque, which is one of the important causes of AD, will be accompanied by an increase in cholinergic activity with enzyme inhibition, and may show a stronger approach in the treatment of AD.

Table 3
Calculated ADME parameters of compounds **P1-P12**.

Compounds	MW	RB	DM	MV	DHB	AHB	PSA	logP	logS	PCaco	logBB	PMDCK	PM	%HOA	VRF	VRT
P1	259.694	4	7.865	849.436	1	3.50	62.269	3.148	−3.928	1331.085	−0.378	1712.056	1	100	0	0
P2	294.140	4	7.305	893.549	1	3.50	62.271	4.086	−4.472	1331.011	−0.223	4223.608	1	100	0	0
P3	275.694	5	9.319	872.606	2	4.25	84.951	2.616	−4.102	400.952	−0.983	468.011	2	88.854	0	0
P4	273.721	4	8.082	908.374	1	3.50	62.269	3.388	−4.846	1331.085	−0.403	1712.056	2	100	0	0
P5	304.692	5	10.139	931.836	1	4.50	110.935	2.644	−4.518	136.807	−1.516	146.387	2	80.659	0	0
P6	277.685	4	7.294	865.540	1	3.50	62.273	3.278	−4.124	1330.967	−0.271	3095.488	1	100	0	0
P7	319.747	6	8.270	987.996	1	5.00	78.941	3.293	−4.474	1331.086	−0.526	1712.057	3	100	0	0
P8	328.585	4	8.841	933.851	1	3.50	62.270	4.311	−5.258	1331.051	−0.093	8797.940	1	100	0	0
P9	319.747	7	8.324	1014.580	2	5.00	92.247	2.965	−4.733	427.815	−1.185	501.992	3	91.402	0	0
P10	317.731	5	5.336	1001.975	1	5.50	97.223	2.902	−4.791	419.272	−1.056	491.167	1	90.874	0	0
P11	302.763	5	7.895	1016.485	1	4.50	64.925	3.688	−5.126	1331.084	−0.504	1712.054	2	100	0	0
P12	305.720	6	8.535	942.229	2	5	92.765	2.631	−4.105	427.815	−1.036	501.992	3	89.446	0	0

2.3. Prediction of physicochemical parameters

A drug candidate compound must have acceptable physicochemical and pharmacokinetic properties to be eligible for further clinical testing. Estimates of the absorption, distribution, metabolism, excretion and toxicity (ADMET) allow early detection of problems related to the formulation, drug safety and prevent increased drug development costs or time [31,32]. Therefore, the evaluation of the ADME properties is beneficial and important in the drug development process.

A compound must cross the blood-brain barrier to be able to exhibit its AChE inhibitory activity [6]. The LogP and LogBB parameters, calculated for this purpose and predicting blood brain barrier crossing, were within the accepted range for all compounds.

The PCaco and PMDCK parameters play critical roles in the determination of *in vitro* absorption. The PCaco and PMDCK values of compounds **P3, P5, P9, P10** and **P12** were within the recommended limits. The druglikeness properties of the compounds, such as Lipinski's rule of five and Jorgensen's rule of three, were also evaluated. All compounds were in accordance with the accepted range and they did not show any violations. The calculated ADME parameters of synthesized compounds were presented in Table 3.

MW: Molecular weight **RB:** Number of rotatable bonds (recommended value: 0–15) **DM:** Computed dipole moment (recommended value: 1–12.5) **MV:** Total solvent-accessible volume (recommended value: 500–2000) **DHB:** Estimated number of hydrogen bond donors (recommended value: 0–6) **AHB:** Estimated number of hydrogen bond acceptors (recommended value: 2–20) **PSA:** Van der Waals surface area of polar nitrogen and oxygen atoms and carbonyl carbon atoms (recommended value: 7–200) **logP:** Predicted octanol/water partition coefficient (recommended value: −2–6.5) **logS:** Predicted aqueous solubility (recommended value: −6.5–0.5) **PCaco:** Predicted apparent Caco-2 cell permeability (recommended value: <25 poor, >500 great) **logBB:** Predicted brain/blood partition coefficient (recommended value: −3–1.2) **PMDCK:** Predicted apparent MDCK cell permeability (recommended value: <25 poor, >500 great) **PM:** Number of likely metabolic reactions (recommended value: 1–8)**%HOA:** Predicted human oral absorption percent (recommended value: >80% is high, <25% is poor) **VRF:** Number of violations of Lipinski's rule of five. The rules are: MW < 500, logP < 5, DHB ≤ 5, AHB ≤ 10, Positive PSA value. **VRT:** Number of violations of Jorgensen's rule of three. The three rules are: logS > −5.7, PCaco > 22 nm/s, PM < 7.

Some adverse effects such as hepatotoxicity of AChE inhibitors used in the clinic have been reported [10]. For example tacrine, the first approved AChE inhibitor, was withdrawn from use due to its serious hepatotoxic adverse effects [33]. Therefore, the potential cytotoxic activity of AChE inhibitors must be investigated. As a matter of fact, the mutagenic, tumorigenic, reproductive and irritant effects of the synthesized compounds were evaluated by *in silico* methods in this study. None of the synthesized compounds showed mutagenic, tumorigenic, reproductive and irritant effects (compound **P11** may only have tumorigenic activity). In addition, for the evaluation of drug efficacy and safety, the hERG Blockers and H–HT parameters of synthesized compounds were assessed by *in silico* methods. The hERG plays a major role in the regulation of the exchange of cardiac action potential and resting potential. The H–HT parameter also demonstrates the potential hepatotoxicity of compounds. It was determined that all synthesized compounds did not violate these hERG Blockers and H–HT parameters. It was also found that the compounds did not have acute toxicity during oral administration (Supplementary File **Table S2**).

As a result of the ADMET and BBB permeability studies, the synthesized compounds have good pharmacokinetic profiles and exhibit high BBB penetration that may be appropriate for clinical use in CNS disorders.

2.4. Evaluation of molecular docking studies

2.4.1. Molecular docking studies of AChE enzyme

In order to determine the possible interactions of compounds **P5, P7, P9** and **P12** with the enzyme active site, which had high AChE enzyme inhibition activity, docking studies were carried out on the crystal structure of the AChE enzyme (PDB Code: 4EY7) [34].

When the AChE enzyme structure is examined, it is striking that it has two different binding sites: the catalytic site (CAS) and the peripheral anionic site (PAS). It has been reported that amino acids Trp86, Gly122, Tyr130, Tyr133, Ser203, Glu334, Tyr337, Phe338 and His447 are effective in binding to the CAS region; while Tyr72, Asp74, Tyr124, Trp286, Phe295 and Tyr341 amino acids are required to bind to the PAS region [34–38]. It was determined in many modeling studies that donepezil interacted with both regions of the AChE enzyme and settled very well in the gorge with its dual binding side-DBS feature [39–41].

The rendered docking poses of the active agents **P5, P7, P9** and **P12** were given in Figs. 3 and 4. It was seen from these poses that the related derivatives were settled in the gorge formed by both CAS and PAS regions together and exerted their effects. Similar to the donepezil molecule, the related compounds interacted with the double binding sites (DBS) and settled on the active site of the enzyme (Fig. 3).

Molecular modeling studies on donepezil showed that the π-π interaction between the indanone ring and the indole ring of Trp286 amino acid was important for binding to the PAS region of the enzyme active site [34,39–41]. The fact that this interaction was observed between Trp286 with 6-chloropyridine of compounds **P5, P7, P9** and **P12** in the experiments indicated that the chosen method and the path followed were correct in terms of the

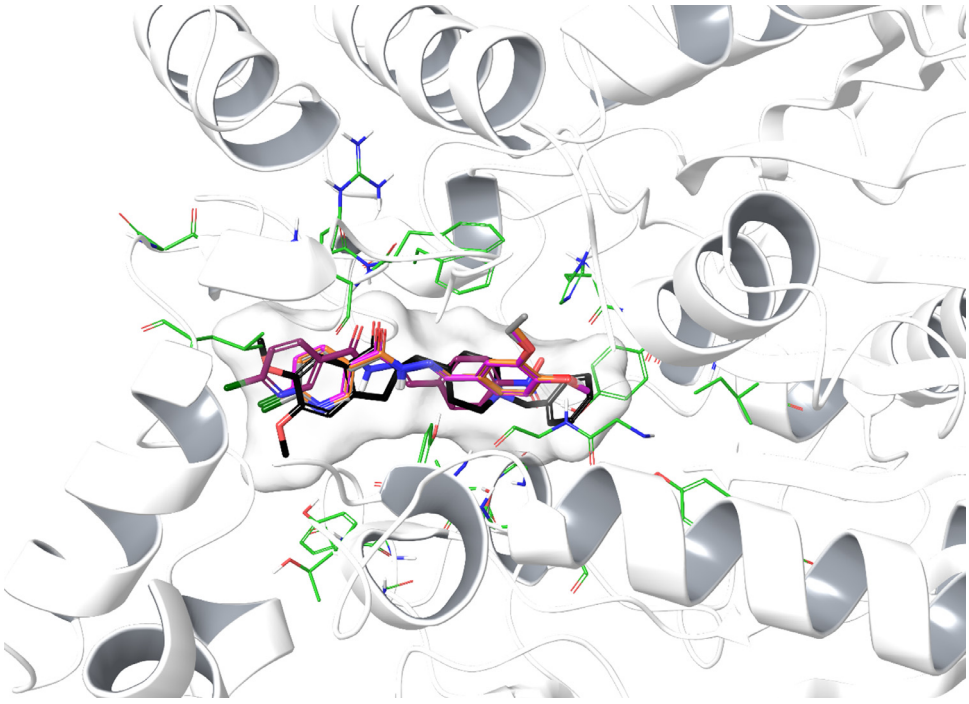

Fig. 3. The superimposition pose of donepezil (black), compounds **P5** (maroon), **P7** (pink), **P9** (gray) and **P12** (orange) in the enzyme active site of AChE enzyme (PDB Code: 4EY7).

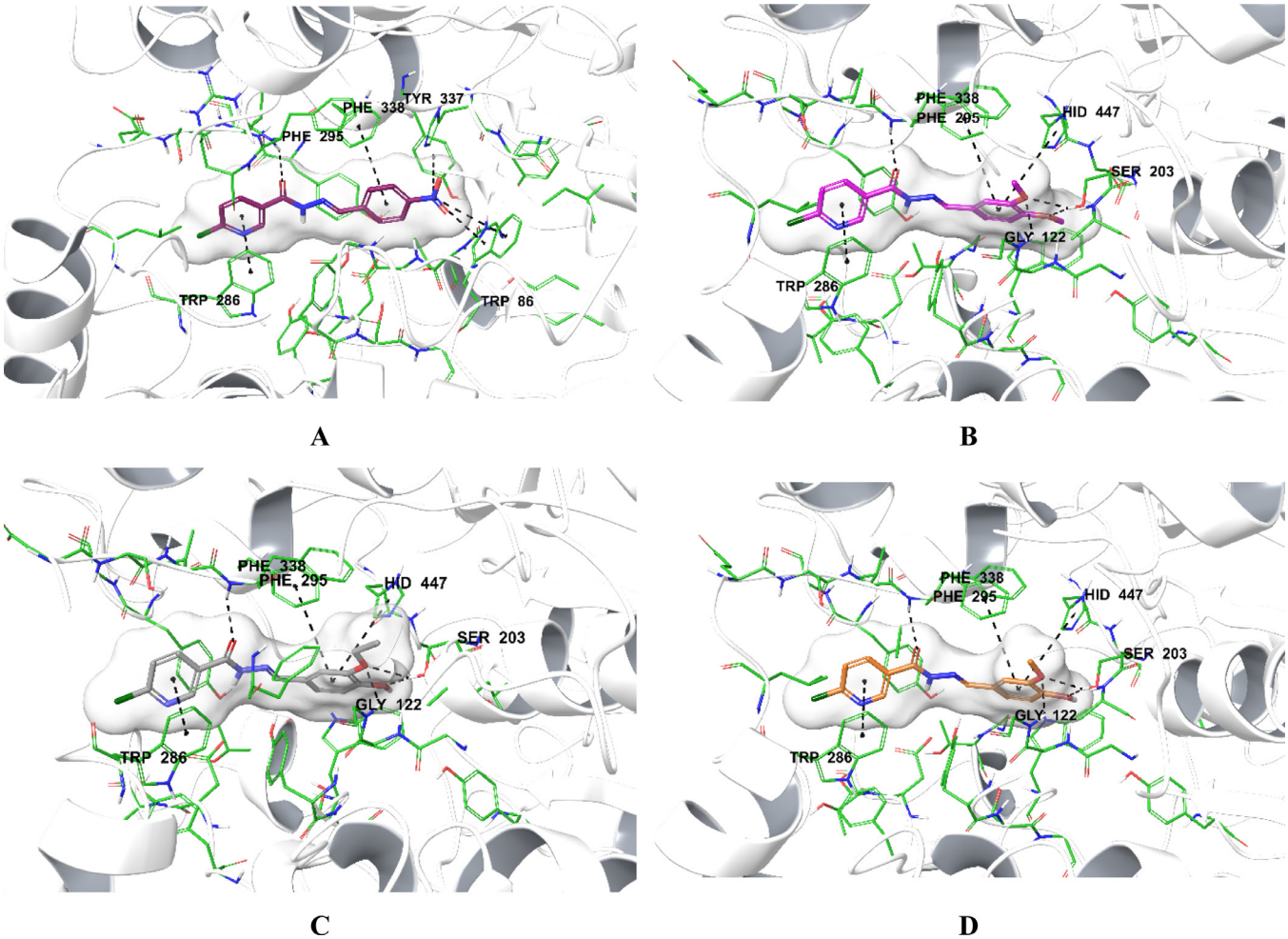

Fig. 4. The 3D interacting modes of compounds **P5** (A), **P7** (B), **P9** (C) and **P12** (D) in the active region of the AChE enzyme (PDB Code: 4EY7). Compounds **P5**, **P7**, **P9** and **P12** were shown in tube models and maroon, pink, gray and orange-colored, respectively.

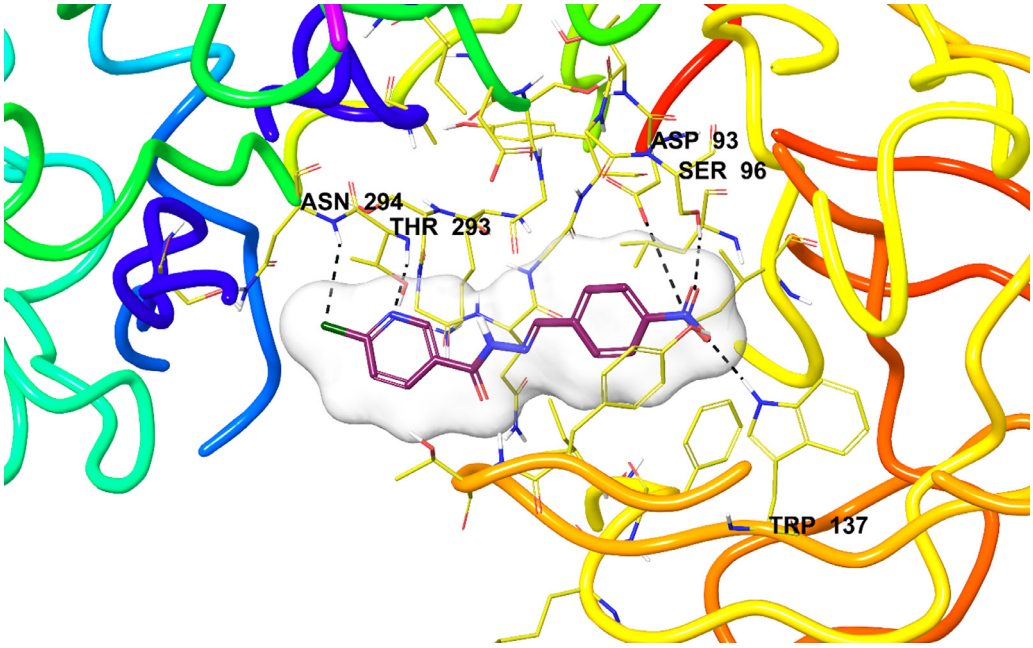

Fig. 5. The 3D interacting mode of compound **P5** in the active region of BACE-1 enzyme (PDB Code: 5HU1). Compound **P5** was shown in a tube model and maroon color.

docking procedure. Another interaction related to the PAS region was detected between the carbonyl near to 6-chloropyridine ring and the amine of Phe295 (Fig. 4-**A, B, C, D**). All these observed interactions were very important as they showed that the related compounds bind to the PAS region.

When analyzing the docking poses (Fig. 4-**A, B, C, D**) in terms of the interactions related to the CAS region, similar common interactions were observed in all tested compounds. In compounds **P5, P7, P9** and **P12**, the substituted phenyl ring near to hydrazine group formed a π-π interaction with the phenyl of Phe338. Also, this phenyl ring in the derivatives **P7, P9** and **P12** created additionally another π-π interaction with the imidazole of Hid447. The main chemical structural difference of compounds **P5, P7, P9** and **P12** was the various substituents of this phenyl ring. Compound **P5** had a nitro group at the 4th position of the phenyl and it was seen that it formed three cation-π interactions with the phenyl of Tyr337 and indole of Trp86 owing to its nitrogen atom. Derivatives **P7, P9** and **P12** bore the substituents at the 3rd and 4th positions different than that of compound **P5**. Compound **P7** had dimethoxy moiety; while compounds **P9** and **P12** had ethoxy/methoxy at the 3rd position and a hydroxyl group at the 4th position. The related substituents of three compounds were very convenient to form hydrogen bonds by acting as a hydrogen acceptor and donor. It was detected from the docking poses that these substituents of compounds **P7, P9** and **P12** displayed the same hydrogen bonds. These substituents established three hydrogen bond formations with the amino of Gly122 and hydroxyl of Ser203.

Consequently, molecular docking studies have shown that the substituents capable of formation of a hydrogen bond at the 3rd and 4th positions of the phenyl ring in compounds **P7, P9** and **P12** contribute positively to enzyme activity. Moreover, the reason why compound **P5** was more active than compounds **P7, P9** and **P12** was that it had additional interactions belonging to the nitro group at the para-position of the phenyl ring. According to the findings of the enzyme inhibition, the electron-withdrawing groups such as nitro moiety was assumed to have contributed positively to enzyme inhibition ability on the AChE enzyme.

2.4.2. Molecular docking studies of BACE-1 enzyme

As mentioned in the BACE-1 inhibitory activity assay, compound **P5** was found to be the most active agent in the selected compounds on the BACE-1 enzyme. To further understand the binding mode of this derivative with BACE-1, the docking simulation study was performed using the X-ray crystal structure of BACE-1 (PDB: 5HU1) [42,43].

The docking results confirmed that the nitrogen atom of the nitro group at the 4th position of the phenyl ring formed a hydrogen bond with the hydroxyl of Asp93 at the central catalytic site of BACE-1. Also, it was seen that compound **P5** could occupy the contiguous S1 and S3 pockets (Fig. 5). Moreover, the other hydrogen bond formations related to the oxygen atoms of the nitro group were observed with the hydroxyl of Ser96 and nitrogen of the indole ring of Trp137. The last interactions were detected on the other end of the chemical structure. 6-Chloropyridine ring displayed a halogen bond with the amine of Asn294 owing to the chlorine atom. Also, the nitrogen atom of pyridine formed another hydrogen bond with the amine of Thr293. All obtained these interactions explained that compound **P5** settle very properly in the active site of BACE-1 and why it showed significant *in vitro* enzyme inhibitory activity.

3. Experimental

3.1. Chemistry

All chemicals were purchased from Sigma-Aldrich or Merck. Melting points were determined on a Kleinfield SMP II apparatus and are uncorrected. Thin layer chromatography (TLC, Merck 60 F254) on silica gel F254 (Merck) plates (0.25 mm thickness) was used to monitor the progress of the reaction. The IR spectra were recorded using a Shimadzu FTIR 8400S spectrometry. The NMR spectra were recorded on a Bruker Fourier 300 (Bruker Bioscience, Billerica, MA, USA), operating at 300 MHz (^{1}H NMR) and 75 MHz (^{13}C NMR). Elemental analysis was performed on the Leco CHNS-932 analyzer.

3.1.1. General synthesis procedure for hydrazide compound

Methyl 6-chloropyridine-3-carboxylate (0.01 mol) was taken into a flask in 20 ml of ethanol. Hydrazine monohydrate (8 ml, 98%) was added to the mixture and heated on a water bath for 6–8 h. After the completion of the reaction, the precipitate was separated from the solution by filtration, dried and crystallized from methanol [44].

Yield: 80%; m.p. 224–225 °C. IR (ν, cm^{-1}): 3446, 3196 (N–H), 3061 (aromatic =C–H), 1651 (C=O), 1602 (C=N, pyridine), 1062 (aromatic C–Cl). ^{1}H NMR (300 MHz, DMSO–d_6, ppm): δ 4.59 (s, 2H, NH_2), 7.65 (d, J = 8.1 Hz, 1H, pyridine meta proton), 8.21 (d, J = 8.1 Hz, 1H, pyridine para proton), 8.80 (d, 1H, J = 2.4 Hz, pyridine orto proton), 10.03 (s, 1H, NH). Anal. Calcd for $C_6H_6ClN_3O$: C 42.00, H 3.52, N 24.49. Found: C 42.10, H 3.55, N 24.41%.

3.1.2. General synthesis procedure for hydrazone compounds (P1-P12)

Hydrazide compound (*6-chloronicotinohydrazide*) (1 mmol) and equimolar quantities of benzaldehyde derivatives (1 mmol) were taken into a round bottom flask. Methanol (15 ml) was added to the mixture and refluxed for 10–12 h. After controlling with TLC, the excess solvent was evaporated under vacuum, the residue was washed with water and crystallized from ethanol [45].

*N'-Benzylidene-6-chloronicotinohydrazide (**P1**)*

Yield: 80%; m.p. 201.4–201.6 °C. IR (ν, cm^{-1}): 3352, 3190 (N–H), 3020 (aromatic =C–H), 1645 (C=O), 1633 (C=N, hydrazone), 1602 (C=N, pyridine), 1097 (aromatic C–Cl). ^{1}H NMR (300 MHz, DMSO–d_6, ppm): δ 7.42–7.77 (m, 6H, Ar-H), 8.33 (d, J = 8.4 Hz, 1H, pyridine para proton), 8.45 (s, 1H, NH), 8.92 (d, 1H, J = 2.1 Hz, pyridine orto proton), 12.07 (s, 1H, -N=CH). ^{13}C NMR (100 MHz, DMSO–d_6, ppm): δ 123.67, 124.28, 126.86, 127.24, 128.56, 128.88, 130.35, 134.00, 139.00, 148.72, 149.18 (C=N), 152.93 (C=N), 160.60 (C=O). Anal. Calcd. for $C_{13}H_{10}ClN_3O$: C 60.12, H 3.88, N 16.18. Found: C 60.10, H 3.90, N 16.25%.

6-Chloro-N'-(4-chlorobenzylidene)nicotinohydrazide (**P2**)

Yield: 80%; m.p. 200.0–200.3 °C. IR (ν, cm^{-1}): 3144 (N–H), 3003 (aromatic =C–H), 1697 (C=O), 1633 (C=N, hydrazone), 1606 (C=N, pyridine), 1057 (aromatic C–Cl). ^{1}H NMR (300 MHz, DMSO–d_6, ppm): δ 7.53 (d, J = 8.7 Hz, 2H, Ar-H), 7.66 (d, J = 8.4 Hz, 1H, pyridine meta proton), 7.77 (d, J = 8.7 Hz, 2H, Ar-H), 8.30 (d, J = 8.7 Hz, 1H, pyridine para proton), 8.42 (s, 1H, NH), 8.91 (d, 1H, J = 2.4 Hz, pyridine orto proton), 12.14 (s, 1H, -N=CH). ^{13}C NMR (100 MHz, DMSO–d_6, ppm): δ 123.72, 124.30, 128.87, 128.99, 130.01, 132.96, 134.80, 139.03, 140.76, 147.32, 149.22 (C=N), 152.99 (C=N), 160.64 (C=O). Anal. Calcd. for $C_{13}H_9Cl_2N_3O$: C 53.08, H 3.08, N 14.29. Found: C 53.20, H 3.11, N 14.19%.

6-Chloro-N'-(4-hydroxybenzylidene)nicotinohydrazide (**P3**)

Yield: 80%; m.p. 196.9–197.2 °C. IR (ν, cm^{-1}): 3524 (O–H), 3190 (N–H), 3055 (aromatic =C–H), 1680 (C=O), 1620 (C=N, hydrazone), 1599 (C=N, pyridine), 1303 (C–O), 1055 (aromatic C–Cl). ^{1}H NMR (300 MHz, DMSO–d_6, ppm): δ 6.83 (d, J = 8.4 Hz, 2H, Ar-H), 7.60 (d, J = 8.7 Hz, 1H, pyridine meta proton), 7.69 (d, J = 8.4 Hz, 2H, Ar-H), 8.30 (d, J = 8.7 Hz, 1H, pyridine para proton), 8.32 (s, 1H, NH), 8.89 (d, 1H, J = 2.4 Hz, pyridine orto proton), 10.01 (s, 1H, OH), 11.87 (s, 1H, -N=CH). ^{13}C NMR (100 MHz, DMSO–d_6, ppm): δ 115.74, 123.61, 124.22, 124.96, 128.74, 129.04, 138.91, 140.74, 145.08, 149.09 (C=N), 152.76 (C=N), 160.24 (C=O). Anal. Calcd. for $C_{13}H_{10}ClN_3O_2$: C 56.64, H 3.66, N 15.24. Found: C 56.79, H 3.64, N 15.33%.

6-Chloro-N'-(4-methylbenzylidene)nicotinohydrazide (**P4**)

Yield: 80%; m.p. 192.8–193.4 °C. IR (ν, cm^{-1}): 3149 (N–H), 3030 (aromatic =C–H), 2845 (C–H asym.), 2731 (C–H sym.), 1666 (C=O), 1633 (C=N, hydrazone), 1602 (C=N, pyridine), 1058 (aromatic C–Cl). ^{1}H NMR (300 MHz, DMSO–d_6, ppm): δ 2.31 (s, 3H, CH_3), 7.27 (d, J = 8.1 Hz, 2H, Ar-H), 7.64 (d, J = 8.1 Hz, 1H, pyridine meta proton), 7.70 (d, J = 8.4 Hz, 2H, Ar-H), 8.30 (d, J = 8.4 Hz, 1H, pyridine para proton), 8.39 (s, 1H, NH), 8.90 (d, 1H, J = 2.4 Hz, pyridine orto proton), 12.01 (s, 1H, -N=CH). ^{13}C NMR (100 MHz, DMSO–d_6, ppm): δ 21.07 (CH_3), 123.69, 124.29, 126.88, 127.25, 128.63, 129.51, 131.31, 139.01, 140.26, 148.72, 149.20 (C=N), 152.90 (C=N), 160.49 (C=O). Anal. Calcd. for $C_{14}H_{12}ClN_3O$: C 61.43, H 4.42, N 15.35. Found: C 61.29, H 4.38, N 15.29%.

6-Chloro-N'-(4-nitrobenzylidene)nicotinohydrazide (**P5**)

Yield: 80%; m.p. 236.6–237.0 °C. IR (ν, cm^{-1}): 3419 (N–H), 3053 (aromatic =C–H), 1660 (C=O), 1640 (C=N, hydrazone), 1612 (C=N, pyridine), 1516 (NO_2 asym.), 1317 (NO_2 sym.), 1072 (aromatic C–Cl). ^{1}H NMR (300 MHz, DMSO–d_6, ppm): δ 7.72 (d, J = 8.4 Hz, 1H, pyridine meta proton), 8.01 (d, J = 8.4 Hz, 2H, Ar-H), 8.14 (d, J = 8.4 Hz, 2H, Ar-H), 8.30 (d, J = 8.7 Hz, 1H, pyridine para proton), 8.39 (s, 1H, NH), 8.92 (d, 1H, J = 1.8 Hz, pyridine orto proton), 12.36 (s, 1H, -N=CH). ^{13}C NMR (125 MHz, DMSO–d_6, ppm): δ 124.52, 124.78, 128.64, 128.78, 130.02, 139.53, 140.78, 146.73, 148.56, 149.74 (C=N), 152.66 (C=N), 160.38 (C=O). Anal. Calcd. for $C_{13}H_9ClN_4O_3$: C 51.25, H 2.98, N 18.39. Found: C 51.35, H 3.00, N 18.32%.

6-Chloro-N'-(4-fluorobenzylidene)nicotinohydrazide (**P6**)

Yield: 80%; m.p. 210.1–210.5 °C. IR (ν, cm^{-1}): 3173 (N–H), 3003 (aromatic =C–H), 1643 (C=O), 1633 (C=N, hydrazone), 1600 (C=N, pyridine), 1107 (aromatic C–Cl). ^{1}H NMR (300 MHz, DMSO–d_6, ppm): δ 7.27 (t, 2H, Ar-H), 7.71 (d, J = 8.1 Hz, 1H, pyridine meta proton), 7.80 (d, J = 8.7 Hz, 2H, Ar-H), 8.32 (d, J = 8.4 Hz, 1H, pyridine para proton), 8.43 (s, 1H, NH), 8.91 (d, 1H, J = 2.1 Hz, pyridine orto proton), 12.08 (s, 1H, -N=CH). ^{13}C NMR (100 MHz, DMSO–d_6, ppm): δ 115.85, 116.07, 124.29, 128.52, 129.41, 130.61, 139.00, 143.65, 147.58, 149.18 (C=N), 152.95 (C=N), 160.60 (C=O), 164.51. Anal. Calcd. for $C_{13}H_9ClFN_3O$: C 56.23, H 3.27, N 15.13. Found: C 56.28, H 3.25, N 15.17%.

6-Chloro-N'-(3,4-dimethoxybenzylidene)nicotinohydrazide (**P7**)

Yield: 80%; m.p. 213.3–213.8 °C. IR (ν, cm^{-1}): 3194 (N–H), 3063 (aromatic =C–H), 2958 (C–H asym.), 2837 (C–H sym.), 1645 (C=O), 1633 (C=N, hydrazone), 1559 (C=N, pyridine), 1309 (C–O), 1138 (aromatic C–Cl). ^{1}H NMR (300 MHz, DMSO–d_6, ppm): δ 3.82 and 3.83 (2 s, 6H, OCH_3), 7.03 (d, J = 8.1 Hz, 1H, Ar-H), 7.22 (d, J = 8.4 Hz, 1H, Ar-H), 7.35 (s, 1H, Ar-H), 7.70 (d, J = 8.1 Hz, 1H, pyridine meta proton), 8.29 (d, J = 8.1 Hz, 1H, pyridine para proton), 8.36 (s, 1H, NH), 8.90 (d, 1H, J = 2.1 Hz, pyridine orto proton), 11.95 (s, 1H, -N=CH). ^{13}C NMR (125 MHz, DMSO–d_6, ppm): δ 55.94 (OCH_3), 56.05 (OCH_3), 108.80, 111.96, 122.60, 124.73, 127.16, 129.19, 139.42, 149.40, 149.59 (C=N), 151.45, 153.29 (C=N), 160.86 (C=O). Anal. Calcd. for $C_{15}H_{14}ClN_3O_3$: C 56.35, H 4.41, N 13.14. Found: C 56.45, H 4.43, N 13.03%.

6-Chloro-N'-(3,4-dichlorobenzylidene)nicotinohydrazide (**P8**)

Yield: 80%; m.p. 195.1–195.6 °C. IR (ν, cm^{-1}): 3213 (N–H), 3066 (aromatic =C–H), 1645 (C=O), 1626 (C=N, hydrazone), 1602 (C=N, pyridine), 1134 (aromatic C–Cl). ^{1}H NMR (300 MHz, DMSO–d_6, ppm): δ 7.67–7.79 (m, 3H, Ar-H and pyridine meta proton), 7.99 (s, 1H, Ar-H), 8.30 (d, J = 8.4 Hz, 1H, pyridine para proton), 8.40 (s, 1H, NH), 8.91 (d, 1H, J = 2.1 Hz, pyridine orto proton), 12.27 (s, 1H, -N=CH). ^{13}C NMR (100 MHz, DMSO–d_6, ppm): δ 124.28, 126.97, 128.30, 128.69, 131.12, 131.74, 132.53, 134.85, 139.04, 145.92, 149.24 (C=N), 153.07 (C=N), 160.78 (C=O). Anal. Calcd. for $C_{13}H_8Cl_3N_3O$: C 47.52, H 2.45, N 12.79. Found: C 47.63, H 2.44, N 12.85%.

6-Chloro-N'-(3-ethoxy-4-hydroxybenzylidene)nicotinohydrazide (**P9**)

Yield: 80%; m.p. 201.1–201.5 °C. IR (ν, cm^{-1}): 3392 (O–H), 3228 (N–H), 3057 (aromatic =C–H), 2978 (C–H asym.), 2887 (C–H sym.), 1633 (C=O), 1612 (C=N), 1315 (C–O), 1101 (aromatic C–Cl). ^{1}H NMR (300 MHz, DMSO–d_6, ppm): δ 1.37 (t, 3H, CH_3), 4.06 (q, 2H, OCH_2), 6.85 (d, J = 8.1 Hz, 1H, Ar-H), 7.13 (d, J = 8.1 Hz, 1H, Ar-H), 7.31 (s, 1H, Ar-H), 7.69 (d, J = 8.4 Hz, 1H, pyridine meta proton), 8.27 (d, J = 8.1 Hz, 1H, pyridine para proton), 8.37 (s, 1H, NH), 8.89 (d,

1H, J = 2.1 Hz, pyridine orto proton), 9.54 (s, 1H, OH), 11.90 (s, 1H, -N=CH). ^{13}C NMR (125 MHz, DMSO–d_6, ppm): δ 15.18 (CH_3), 64.36 (OCH_2), 110.93, 116.03, 122.76, 124.71, 129.23, 139.40, 147.67, 149.57, 149.75, 149.98 (C=N), 153.25 (C=N), 160.76 (C=O). Anal. Calcd. for $C_{15}H_{14}ClN_3O_3$: C 56.35, H 4.41, N 13.14. Found: C 56.27, H 4.38, N 13.07%.

*6-Chloro-N'-(4-carbmethoxybenzylidene)nicotinohydrazide (**P10**)*

Yield: 80%; m.p. 237.3–237.6 °C. IR (ν, cm^{-1}): 3202 (N–H), 3022 (aromatic =C–H), 2945 (C–H asym.), 2856 (C–H sym.), 1635 (C=O), 1602 (C=N), 1302 (C–O), 1112 (aromatic C–Cl). ^{1}H NMR (300 MHz, DMSO–d_6, ppm): δ 3.88 (s, 3H, OCH_3), 7.72 (d, J = 8.4 Hz, 1H, pyridine meta proton), 7.91 (d, J = 8.4 Hz, 2H, Ar-H), 8.06 (d, J = 8.4 Hz, 2H, Ar-H), 8.32 (d, J = 8.4 Hz, 1H, pyridine para proton), 8.44 (s, 1H, NH), 8.92 (d, 1H, J = 2.4 Hz, pyridine orto proton), 12.25 (s, 1H, -N=CH). ^{13}C NMR (100 MHz, DMSO–d_6, ppm): δ 52.11 (OCH_3), 124.17, 127.25, 128.31, 129.53, 130.61, 138.34, 138.90, 147.22, 149.13 (C=N), 152.96 (C=N), 160.67 (C=O), 165.67 (C=O). Anal. Calcd for $C_{15}H_{12}ClN_3O_3$: C 56.70, H 3.81, N 13.23. Found: C 56.65, H 3.82, N 13.20%.

*6-Chloro-N'-(4-(dimethylamino)benzylidene)nicotinohydrazide (**P11**)*

Yield: 80%; m.p. 200.5–200.7 °C. IR (ν, cm^{-1}): 3159 (N–H), 3030 (aromatic =C–H), 2887 (C–H asym.), 2814 (C–H sym.), 1645 (C=O), 1599 (C=N), 1410 (C–N), 1101 (aromatic C–Cl). ^{1}H NMR (300 MHz, DMSO–d_6, ppm): δ 2.98 (s, 6H, $N(CH_3)_2$), 6.75 (d, J = 9.0 Hz, 2H, Ar-H), 7.54 (d, J = 9.0 Hz, 2H, Ar-H), 7.69 (d, J = 8.7 Hz, 1H, pyridine meta proton), 8.27 (d, J = 8.7 Hz, 1H, pyridine para proton), 8.36 (s, 1H, NH), 8.89 (d, 1H, J = 2.4 Hz, pyridine orto proton), 11.78 (s, 1H, -N=CH). ^{13}C NMR (100 MHz, DMSO–d_6, ppm): δ 40.33 (CH_3), 111.76, 121.16, 123.56, 124.20, 128.15, 128.60, 128.88, 138.86, 140.73, 149.03, 149.52 (C=N), 151.67, 152.63 (C=N), 160.01 (C=O). Anal. Calcd for $C_{15}H_{15}ClN_4O$: C 59.51, H 4.99, N 18.51. Found: C 59.62, H 4.97, N 18.58%.

*6-Chloro-N'-(4–hydroxy-3-methoxybenzylidene)nicotinohydrazide (**P12**)*

Yield: 80%; m.p. 223.8–224.3 °C. IR (ν, cm^{-1}): 3481 (O–H), 3174 (N–H), 3047 (aromatic =C–H), 2887 (C–H asym.), 2806 (C–H sym.), 1645 (C=O), 1633 (C=N), 1319 (C–O), 1168 (aromatic C–Cl). ^{1}H NMR (300 MHz, DMSO–d_6, ppm): δ 3.84 (s, 3H, OCH_3), 6.82 (d, J = 8.1 Hz, 1H, Ar-H), 7.10 (s, 1H, Ar-H), 7.33 (d, J = 8.1 Hz, 1H, Ar-H), 7.70 (d, J = 8.4 Hz, 1H, pyridine meta proton), 8.28 (d, J = 8.4 Hz, 1H, pyridine para proton), 8.33 (s, 1H, NH), 8.89 (d, 1H, J = 2.4 Hz, pyridine orto proton), 9.64 (s, 1H, OH), 11.91 (s, 1H, -N=CH). ^{13}C NMR (125 MHz, DMSO–d_6, ppm): δ 56.04 (OCH_3), 109.57, 115.93, 123.94, 124.72, 125.84, 129.22, 139.41, 141.32, 148.53, 149.56, 149.75 (C=N), 153.25 (C=N), 160.79 (C=O). Anal. Calcd for $C_{14}H_{12}ClN_3O_3$: C 55.00, H 3.96, N 13.74. Found: C 55.12, H 3.98, N 13.77%.

3.2. Biological activity studies

3.2.1. In vitro *ChE enzymes inhibition assay*

AChE and BChE inhibitory activities of the synthesized compounds were assessed using the modified Ellman method, as described in the previous studies published by our team [27–30,46,47]. Human acetylcholinesterase (CAS No: 9000–81–1) and human butyrylcholinesterase (CAS No: 9001–08–5) enzymes were used as enzymes in the assay.

3.2.2. In vitro *human β-Secretase (BACE-1) enzyme inhibitor screening assay*

The experimental procedure was based on the "Human β-Secretase (BACE-1) Inhibitor Screening Assay" kit (BioVision, Milpitas, CA, USA) protocol based on the fluorometric method [48].

3.2.3. *Beta-amyloid 1–42 (Aβ42) inhibitor screening assay*

The experimental procedure was based on the "Beta-Amyloid 1–42 (Aβ42) Ligand Screening Assay" kit (BioVision, Milpitas, CA, USA) protocol based on the fluorometric method [29,30].

3.3. Prediction of physicochemical parameters

The physicochemical and pharmacokinetic profiles of synthesized compounds were determined by Schrödinger *QikProp* 4.8 software [49]. Additionally, in order to evaluate toxicological molecular properties, osiris property explorer and ADMETlab 2.0 server were used [50,51].

3.4. Molecular docking studies

The structure-based *in silico* docking method was applied to determine possible binding and interaction points of the most active compounds **P5, P7, P9** and **P12** in the series with the active site of the AChE enzyme. For this purpose, protein-ligand interaction analysis was performed using the crystal structures AChE (PDB: 4EY7) [34]. Also, as a result of *in vitro* β-Secretase (BACE1) inhibitor screening study, compound **P5** was found to be the most effective agent and thus it was included into the docking studies about the BACE-1 enzyme. The X-ray crystal structure of BACE-1 (PDB: 5HU1) [42,43] was used in order to perform this.

The crystal structure was first prepared for docking studies with the *Protein Preparation Wizard* protocol in *Schrödinger Suite 2015 Update 2* [52], the bond lengths were adjusted using the OPLS 2005 force field, and the possible charges of the atoms on the charged amino acids under the specified ambient conditions were determined automatically. The compounds were prepared for molecular docking studies using *Ligprep 2.3* module [53]. Grids were generated with *Glide 7.1* [54] and docking runs were performed with the single-precision (SP) docking mode of the same module.

4. Conclusion

Identification of new and effective structures is an important approach in Alzheimer's treatment. Especially, structures that can show activity against Alzheimer's disease by more than one mechanism rather than a single pathway are promising in the way of becoming new medications. Based on this strategy, some new hydrazone derivatives bearing pyridine ring were synthesized in the present study. The significant AChE inhibitory activities of the compounds **P5, P7, P9, P10** and **P12** were found. On the other hand, BACE1 enzyme and beta amyloid plaque inhibition studies, which are important mechanisms in the treatment of Alzheimer's disease, displayed that compound **P5** had the most active derivative in this series. According to molecular docking results, compound **P5** made additional hydrogen bonds with the active sites of AChE and BACE1 enzymes due to carrying electron withdrawing groups such as nitro on the aromatic ring and contributed positively to enzymes inhibition. In addition, the BBB permeability and ADMET studies were also assessed that all compounds meet the need for CNS drug targets. Therefore compound **P5** is a good example to develop new candidates that may be effective in Alzheimer's disease.

Declaration of Competing Interest

The authors declare that they have no known competing financial interests or personal relationships that could have appeared to influence the work reported in this paper.

CRediT authorship contribution statement

Fatih Tok: Conceptualization, Methodology, Investigation, Writing – review & editing. **Begüm Nurpelin Sağlık:** Methodology,

Software, Investigation, Writing – review & editing. **Yusuf Özkay:** Visualization, Writing – review & editing. **Zafer Asım Kaplancıklı:** Visualization, Data curation. **Bedia Koçyiğit-Kaymakçıoğlu:** Visualization, Data curation.

Acknowledgments

This study was supported by the Marmara University Scientific Research Projects Commission under grant number: SAG-K-130319–0090.

Supplementary materials

Supplementary material associated with this article can be found, in the online version, at doi:10.1016/j.molstruc.2022.133441.

References

[1] D.S. Knopman, H. Amieva, R.C. Petersen, G. Chetelat, D.M. Holtzman, B.T. Hyman, R.A. Nixon, D.T. Jones, Alzheimer disease, Nat. Rev. Dis. Primers 33 (2021) 1–21, doi:10.1038/s41572-021-00269-y.
[2] C.L. Masters, R. Bateman, K. Blennow, C.C. Rowe, R.A. Sperling, J.L. Cummings, Alzheimer's disease, Nat. Rev. Dis. Primers 1 (2015) 1–18, doi:10.1038/nrdp.2015.56.
[3] M. Citron, Alzheimer's disease: strategies for disease modification, Nat. Rev. Drug Discov. 9 (2010) 387–398, doi:10.1038/nrd2896.
[4] J. Wang, B.J. Gu, C.L. Masters, Y.J. Wang, A systemic view of Alzheimer disease - insights from amyloid–β metabolism beyond the brain, Nature 13 (2017) 612–623, doi:10.1038/nrneurol.2017.111.
[5] H. Hampel, M.M. Mesulam, A.C. Cuello, M.R. Farlow, E. Giacobini, G.T. Grossberg, A.S. Khachaturian, A. Vergallo, E. Cavedo, P.J. Snyder, Z.S. Khachaturian, The cholinergic system in the pathophysiology and treatment of Alzheimer's disease, Brain 141 (2018) 1917–1933, doi:10.1093/brain/awy132.
[6] A. Trang, P.B. Khandhar, Physiology, Acetylcholinesterase. [Updated 2021 May 9]. In: StatPearls [Internet], Treasure Island (FL): StatPearls Publishing, 2022 Jan-. Available from https://www.ncbi.nlm.nih.gov/books/NBK539735/ .
[7] M.G. Lionetto, R. Caricato, A. Calisi, M.E. Giordano, T. Schettino, Acetylcholinesterase as a biomarker in environmental and occupational medicine: new insights and future perspectives, Biomed. Res. Int 2013 (2013) 1–9, doi:10.1155/2013/321213.
[8] J.M. Long, D.M. Holtzman, Alzheimer disease: an update on pathobiology and treatment strategies, Cell 179 (2019) 312–339, doi:10.1016/j.cell.2019.09.001.
[9] J.L. Borioni, V. Cavallaro, A.P. Murray, A.B. Penenory, M. Puiatti, M.E. Garcia, Design, synthesis and evaluation of cholinesterase hybrid inhibitors using a natural steroidal alkaloid as precursor, Bioorg. Chem. 111 (2021) 104893, doi:10.1016/j.bioorg.2021.104893.
[10] K. Sharma, Cholinesterase inhibitors as Alzheimer's therapeutics, Mol. Med. Rep. 20 (2019) 1479–1487, doi:10.3892/mmr.2019.10374.
[11] M.A. Ullah, F.T. Johora, B. Sarkar, Y. Araf, N. Ahmed, A.N. Nahar, T. Akter, Computer-assisted evaluation of plantderived β-secretase inhibitors in Alzheimer's disease, Egypt, J. Med. Hum. Genet. 22 (26) (2021) 1–15, doi:10.1186/s43042-021-00150-3.
[12] J. Zhao, X. Liu, W. Xia, Y. Zhang, C. Wang, Targeting amyloidogenic processing of APP in Alzheimer's disease, Front. Mol. Neurosci. 13 (137) (2020) 1–17, doi:10.3389/fnmol.2020.00137.
[13] M.A. DeTure, D.W. Dickson, The neuropathological diagnosis of Alzheimer's disease, Mol. Neurodegener. 14 (2019) 1–18, doi:10.1186/s13024-019-0333-5.
[14] A.K. Ghosh, H.L. Osswald, BACE1 (β-Secretase) inhibitors for the treatment of Alzheimer's disease, Chem. Soc. Rev. 43 (19) (2014) 6765–6813, doi:10.1039/c3cs60460h.
[15] U. Neumann, H. Rueeger, R. Machauer, S.J. Veenstra, R.M. Lueoend, M. Tintelnot-Blomley, G. Laue, K. Beltz, B. Vogg, P. Schmid, W. Frieauff, D.R. Shimshek, M. Staufenbiel, L.H. Jacobson, A novel BACE inhibitor NB-360 shows a superior pharmacological profile and robust reduction of amyloid-β and neuroinflammation in APP transgenic mice, Mol. Neurodegener. 10 (44) (2015) 1–15, doi:10.1186/s13024-015-0033-8.
[16] J. Lee, M. Jun, Dual BACE1 and cholinesterase inhibitory effects of phlorotannins from *Ecklonia cava*—An *in vitro* and in silico study, Mar. Drugs 17 (2019) 91, doi:10.3390/md17020091.
[17] M.V.K. Reddy, K.Y. Rao, G. Anusha, G.M. Kumar, A.G. Damu, K.R. Reddy, N.P. Shetti, T.M. Aminabhavi, P.V.G. Reddy, *In-vitro* evaluation of antioxidant and anticholinesterase activities of novel pyridine, quinoxaline and s-triazine derivatives, Environ. Res. 199 (2021) 111320, doi:10.1016/j.envres.2021.111320.
[18] J. Kumar, A. Gill, M. Shaikh, A. Singh, A. Shandilya, E. Jameel, N. Sharma, N. Mrinal, N. Hoda, B. Jayaram, Pyrimidine-triazolopyrimidine and pyrimidine-pyridine hybrids as potential acetylcholinesterase inhibitors for Alzheimer's disease, ChemistrySelect 3 (2018) 736–747, doi:10.1002/slct.201702599.
[19] H.C. Kwong, C.S.C. Kumar, S.H. Mah, Y.L. Mah, T.S. Chia, C.K. Quah, G.K. Lim, S. Chandraju, Crystal correlation of heterocyclic imidazo[1,2-*a*]pyridine analogues and their anticholinesterase potential evaluation, Sci. Rep. 9 (926) (2019) 1–15, doi:10.1038/s41598-018-37486-7.
[20] F. Vafadarnejad, M. Mahdavi, E. Karimpour-Razkenari, N. Edraki, B. Sameem, M. Khanavi, M. Saeedi, T. Akbarzadeh, Design and synthesis of novel coumarin-pyridinium hybrids: *in vitro* cholinesterase inhibitory activity, Bioorg. Chem. 77 (2018) 311–319, doi:10.1016/j.bioorg.2018.01.013.
[21] N. Karaman, Y. Sıcak, T. Taşkın-Tok, M. Öztürk, A. Karaküçük-İyidoğan, M. Dikmen, B. Koçyiğit-Kaymakçıoğlu, E.E. Oruç-Emre, New piperidine-hydrazone derivatives: synthesis, biological evaluations and molecular docking studies as AChE and BChE inhibitors, Eur. J. Med. Chem. 124 (2016) 270–283, doi:10.1016/j.ejmech.2016.08.037.
[22] U. Acar-Çevik, D. Osmaniye, B.N. Sağlık, B. Kaya-Çavuşoğlu, S. Levent, A.B. Karaduman, S. Ilgın, A.Ç. Karaburun, Y. Özkay, Z.A. Kaplancıklı, G. Turan, Multifunctional quinoxaline-hydrazone derivatives with acetylcholinesterase and monoamine oxidases inhibitory activities as potential agents against Alzheimer's disease, Med. Chem. Res. 29 (2020) 1000–1011, doi:10.1007/s00044-020-02541-4.
[23] İ.O. Ateş, A.E. Evren, B.N. Sağlik, L. Yurttaş, New indane derivatives containing 2-hydrazinothiazole as potential acetylcholinesterase and monoamine oxidase-B inhibitors, Z. Naturforsch C. J. Biosci. 76 (2021) 417–424, doi:10.1515/znc-2021-0058.
[24] F. Tok, B.N. Sağlik, Y. Özkay, S. Ilgın, Z.A. Kaplancıklı, Synthesis of new hydrazone derivatives and evaluation of their monoamine oxidase inhibitory activity, B. Koçyiğit-Kaymakçıoğlu, 114 (2021) 105038, doi:10.1016/j.bioorg.2021.105038.
[25] Q. Li, S. He, Y. Chen, F. Feng, W. Qu, H. Sun, Donepezil-based multi-functional cholinesterase inhibitors for treatment of Alzheimer's disease, Eur. J. Med. Chem. 158 (2018) 463–477, doi:10.1016/j.ejmech.2018.09.031.
[26] J.S. Lan, T. Zhang, Y. Liu, J. Yang, S.S. Xie, J. Liu, Z.Y. Miao, Y. Ding, Design, synthesis and biological activity of novel donepezil derivatives bearing *N*-benzyl pyridinium moiety as potent and dual binding site acetylcholinesterase inhibitors, Eur. J. Med. Chem. 133 (2017) 184–196, doi:10.1016/j.ejmech.2017.02.045.
[27] B.N. Sağlık, S. Ilgın, Y. Özkay, Synthesis of new donepezil analogues and investigation of their effects on cholinesterase enzymes, Eur. J. Med. Chem. 124 (2016) 1026–1040, doi:10.1016/j.ejmech.2016.10.042.
[28] W. Hussein, B.N. Sağlık, S. Levent, B. Korkut, S. Ilgın, Y. Özkay, Z.A. Kaplancıklı, Synthesis and biological evaluation of new cholinesterase inhibitors for Alzheimer's disease, Molecules 23 (2033) (2018) 1–19, doi:10.3390/molecules23082033.
[29] İ. Ceyhun, Ş. Karaca, D. Osmaniye, B.N. Sağlık, S. Levent, Y. Özkay, Z.A. Kaplancıklı, Design and synthesis of novel chalcone derivatives and evaluation of their inhibitory activities against acetylcholinesterase, Arch. Pharm. (2021) e2100372, doi:10.1002/ardp.202100372.
[30] D. Osmaniye, A.E. Evren, B.N. Sağlık, S. Levent, Y. Özkay, Z.A. Kaplancıklı, Design, synthesis, biological activity, molecular docking, and molecular dynamics of novel benzimidazole derivatives as potential AChE/MAO-B dual inhibitors, Arch Pharm. (2021) e2100450, doi:10.1002/ardp.202100450.
[31] B.N. Sağlık, D. Osmaniye, U. Acar-Çevik, S. Levent, B. Kaya-Çavuşoğlu, Ö. Atlı-Eklioğlu, Y. Özkay, A.S. Koparal, Z.A. Kaplancıklı, Synthesis, *in vitro* enzyme activity and molecular docking studies of new benzylaminesulfonamide derivatives as selective MAO-B inhibitors, J. Enz. Inh. Med. Chem. 35 (1) (2020) 1422–1432, doi:10.1080/14756366.2020.1784892.
[32] B.N. Sağlık, B. Kaya-Çavuşoğlu, U. Acar-Çevik, D. Osmaniye, S. Levent, Y. Özkay, Z.A. Kaplancıklı, Novel 1,3,4-thiadiazole compounds as potential MAO-A inhibitors – design, synthesis, biological evaluation and molecular modelling, RSC Med. Chem. 11 (2020) 1063–1074, doi:10.1039/D0MD00150C.
[33] J. Korabecny, K. Musilek, O. Holas, J. Binder, F. Zemek, J. Marek, M. Pohanka, V. Opletalova, V. Dohnal, K. Kuca, Synthesis and *in vitro* evaluation of N-alkyl-7-methoxytacrine hydrochlorides as potential cholinesterase inhibitors in Alzheimer disease, Bioorg. Med. Chem. Lett. 20 (2010) 6093–6095, doi:10.1016/j.bmcl.2010.08.044.
[34] J. Cheung, M.J. Rudolph, F. Burshteyn, M.S. Cassidy, E.N. Gary, J. Love, M.C. Franklin, J.J. Height, Structures of human acetylcholinesterase in complex with pharmacologically important ligands, J. Med. Chem. 55 (2012) 10282–10286, doi:10.1021/jm300871x.
[35] M. Atanasova, G. Stavrakov, I. Philipova, D. Zheleva, N. Yordanov, I. Doytchinova, Galantamine derivatives with indole moiety: docking, design, synthesis and acetylcholinesterase inhibitory activity, Bioorg. Med. Chem. 23 (2015) 5382–5389, doi:10.1016/j.bmc.2015.07.058.
[36] M.B. Colovic, D.Z. Krstic, T.D. Lazarevic-Pasti, A.M. Bondzic, V.M. Vasic, Acetylcholinesterase inhibitors: pharmacology and toxicology, Curr. Neuropharmacol. 11 (2013) 315–335, doi:10.2174/1570159X11311030006.
[37] H. Dvir, I. Silman, M. Harel, T.L. Rosenberry, J.L. Sussman, Acetylcholinesterase: from 3D structure to function, Chem. Biol. Interact. 187 (2010) 10–22, doi:10.1016/j.cbi.2010.01.042.
[38] M.Y. Wu, G. Esteban, S. Brogi, M. Shionoya, L. Wang, G. Campiani, M. Unzeta, T. Inokuchi, S. Butini, J. Marco-Contelles, Donepezil-like multifunctional agents: design, synthesis, molecular modeling and biological evaluation, Eur. J. Med. Chem. 121 (2016) 864–879, doi:10.1016/j.ejmech.2015.10.001.
[39] M. Alipour, M. Khoobi, A. Foroumadi, H. Nadri, A. Moradi, A. Sakhteman, M. Ghandi, A. Shafiee, Novel coumarin derivatives bearing N-benzyl pyridinium moiety: potent and dual binding site acetylcholinesterase inhibitors, Bioorg. Med. Chem. 20 (2012) 7214–7222, doi:10.1016/j.bmc.2012.08.052.
[40] Z.F. Al-Rashid, R.P. Hsung, A computational view on the significance of E-ring in binding of (+)-arisugacin A to acetylcholinesterase, Bioorg. Med. Chem. Lett. 25 (2015) 4848–4853, doi:10.1016/j.bmcl.2015.06.047.
[41] D. Genest, C. Rochais, C. Lecoutey, J.S.-d.Oliveira Santos, C. Ballandonne, S. Butt-Gueulle, R. Legay, M. Since, P. Dallemagne, Design, synthesis and biological

evaluation of novel indano- and thiaindano-pyrazoles with potential interest for Alzheimer's disease, MedChemComm 4 (2013) 925–931, doi:10.1039/C3MD00041A.
[42] J.D. Scott, S.W. Li, A.P.J. Brunskill, X. Chen, K. Cox, J.N. Cumming, M. Forman, E.J. Gilbert, R.A. Hodgson, L.A. Hyde, Q. Jiang, U. Iserloh, I. Kazakevich, R. Kuvelkar, H. Mei, J. Meredith, J. Misiaszek, P. Orth, L.M. Rossiter, M. Slater, J. Stone, C.O. Strickland, J.H. Voigt, G. Wang, H. Wang, Y. Wu, W.J. Greenlee, E.M. Parker, M.E. Kennedy, A.W. Stamford, Discovery of the 3-imino-1, 2, 4-thiadiazinane 1, 1-dioxide derivative verubecestat (MK-8931)–a β-site amyloid precursor protein cleaving enzyme 1 inhibitor for the treatment of Alzheimer's disease, J. Med. Chem. 59 (2016) 10435–10450, doi:10.1021/acs.jmedchem.6b00307.
[43] L. Qu, L. Ji, C. Wang, H. Luo, S. Li, W. Peng, F. Yin, D. Lu, X. Liu, L. Kong, X. Wang, Synthesis and evaluation of multi-target-directed ligands with BACE-1 inhibitory and Nrf2 agonist activities as potential agents against Alzheimer's disease, Eur. J. Med. Chem. 219 (2021) 113441, doi:10.1016/j.ejmech.2021.113441.
[44] B. Koçyiğit-Kaymakçıoğlu, S.S. Yazıcı, F. Tok, M. Dikmen, S. Engür, E.E. Oruç-Emre, A. İyidoğan, Synthesis and anticancer activity of new hydrazide-hydrazones and their Pd (II) complexes, Lett. Drug Des. Discov 16 (5) (2019) 522–532, doi:10.2174/1570180815666180816124102.
[45] G. Turan-Zitouni, W. Hussein, B.N. Sağlık, A. Tabbi, B. Korkut, Design, synthesis and biological evaluation of novel *N*-pyridyl-hydrazone derivatives as potential monoamine oxidase (MAO) inhibitors, Molecules 23 (2018) 1–12, doi:10.3390/molecules23010113.
[46] F. Tok, B. Koçyiğit Kaymakçıoğlu, B.N. Sağlık, S. Levent, Y. Özkay, Z.A. Kaplancıklı, Synthesis and biological evaluation of new pyrazolone Schiff bases as monoamine oxidase and cholinesterase inhibitors, Bioorg. Chem. 84 (2019) 41–50, doi:10.1016/j.bioorg.2018.11.016.
[47] C. Yamali, F.S. Engin, S. Bilginer, M. Tuğrak, D. Ozmen-Ozgun, G. Ozli, S. Levent, B.N. Sağlık, Y. Özkay, H.İ. Gül, Phenothiazine-based chalcones as potential dual-target inhibitors towards cholinesterases (AChE, BuChE) and monoamine oxidases (MAO-A, MAO-B), J. Het. Chem. 58 (1) (2021) 161–171, doi:10.1002/jhet.4156.
[48] Human β-Secretase(BACE1) Inhibitor Screening Kit (Fluorometric)-Catalog no:K720-100 (BioVision, Milpitas, CA, USA), QikProp. Schrödinger, LLC, New York, NY, USA, 2016 version 4.8.
[49] QikProp. Schrödinger, LLC; New York, NY, USA: 2016. version 4.8.
[50] M. Rashid, Design, synthesis and ADMET prediction of bis-benzimidazole as anticancer agent, Bioorg. Chem. 96 (2020) 103576, doi:10.1016/j.bioorg.2020.103576.
[51] M.R. Antoniyevic, E.H. Avdovic, D.M. Simijonovic, Z.B. Milanovic, A.D. Amic, Z.S. Markovic, Radical scavenging activity and pharmacokinetic properties of coumarin–hydroxybenzohydrazide hybrids, Int. J. Mol. Sci. 23 (2022) 1–16, doi:10.3390/ijms23010490.
[52] L. Schrödinger, LigPrep. version 3 (2016).
[53] S. Release, 2: LigPrep, Version, 3, Schrödinger, LLC, New York, NY, 2016 (2016).
[54] L. Schrödinger, Glide, Version 7.1, Schrödinger, LLC, New York, NY, USA, 2016.